

Measurement of plastic strains by 3D image correlation photogrammetry at the grain scale

Professor Dr. Dierk Raabe, Dipl.-Ing. Michael Sachtleber

*Max-Planck-Institut für Eisenforschung
Max-Planck-Str. 1
40237 Düsseldorf
Germany
(raabe@mpie.de)*



Summary

Polycrystals with columnar coarse grains are plastically compressed in a channel die for imposing an external plane-strain state. The spatial distribution of the accumulated plastic surface strains in the deformed polycrystals is determined by measuring the displacement fields using 3D quantitative image correlation photogrammetry. For this purpose digital stereological image pairs of the sample surface are taken at the beginning and after each deformation step. The displacement field is derived from them by applying an image analysis method based on pattern recognition to the data before and after straining. The three components of the plastic displacement vector field are used to derive the surface portion of the plastic strain tensor field. The microtexture of the specimens is determined by analysis of electron back scattering patterns obtained in a scanning electron microscope. The experiments are interpreted by comparing them to corresponding crystal plasticity finite element simulations.

1. Introduction

Deformed crystalline matter usually reveals a nonuniform distribution of the plastic strain. This can be attributed to the anisotropic nature of crystal slip, to the non-isotropic interaction of the different lattice defects, and to the influence of macroscopic boundary conditions in terms of geometry and friction.

This article reports about a novel experimental approach for the investigation of such phenomena at the grain scale [1-7]. The technique is characterized by the joint application of photogrammetry and microtexture determination [1]. It aims at mapping both, mechanical and crystallographic changes during plastic deformation of polycrystalline aluminium specimens. Photogrammetry is a method to determine the spatial distribution of microstrains at the sample surface by measurement of changes in the three dimensional plastic displacement field during a deformation experiment [1, 8]. The technique consists in employing a pattern recognition algorithm for the detection of changes in the gray scale distribution of surface patterns occurring during elastic-plastic straining. The microtexture of the specimens is determined by analysis of electron back scattering patterns obtained in a scanning electron microscope.

The aim of this project is to better understand the plastic interaction of grains in polycrystalline specimens under loading. Scientific and technological spin-off from such investigations may be expected for the fields of microstructure mechanics of miniaturized crystalline devices; strain localization in polycrystalline aggregates; material failure; surface roughness mechanics; grain cluster mechanics, Taylor-Bishop-Hill type polycrystal homogenization theory; orientation dependence of nano-indentation; and phenomenological theories of nucleation for homo- and heterophase transformations in plastically strained crystalline matter.

2. Experimental

2.1. Basic procedure

The experiments aim at the joint determination of the accumulated nonuniform plastic strain field and the microtexture in the same sample. The data are taken between subsequent plastic deformation steps exerted in a plane-strain channel die set-up.

Coarse grained recrystallized polycrystalline aluminum samples of commercial purity (>99.99 wt.% Al) were used to prepare the specimens. A quasi-two dimensional array of crystals with columnar morphology perpendicular to the transverse sample surface was prepared by heating samples into the grain growth and subsequent tertiary recrystallization regime. The final average grain size was about 3.5 mm. After annealing each specimen was polished and finally etched. The sample shape was limited by the size of the chamber of the scanning electron microscope and by the 70° tilting angle required for obtaining Kikuchi backscatter diffraction patterns for the determination of the microtexture. Taking into account the elongation of the sample during plane strain deformation a maximum sample size of 17 mm × 10 mm and a thickness between from 3 mm and 10 mm was chosen. These limitations in sample size were necessary to mount the elongated sample into the scanning microscope for microtexture analysis between the subsequent deformation steps.

Prior to the first deformation step crystal orientation maps were taken at the sample surface. Orientation mapping is a technique for analyzing the topology of texture and grain boundaries in crystalline material. Local lattice orientations are measured on a regular grid by automated acquisition and processing of electron backscatter diffraction patterns in the scanning electron microscope. The microstructure can subsequently be reconstructed by coloring similar orientations on the measured grid with similar colors. In addition the pattern quality of the Kikuchi patterns which is a measure for the local perfection of the crystal lattice is determined for each point. In the present investigation the size of the measurement grid was chosen as compromise between accuracy and measuring time. The grid step size was 100 µm which is well below the average grain size of 3500 µm.

After determination of the starting texture plane strain compression experiments were conducted. For this purpose a servo-hydraulic mechanical testing machine equipped with a



channel die set-up was used. The tools were made from hardened steel and consisted of three parts which were bolted together during the test (Fig. 1).

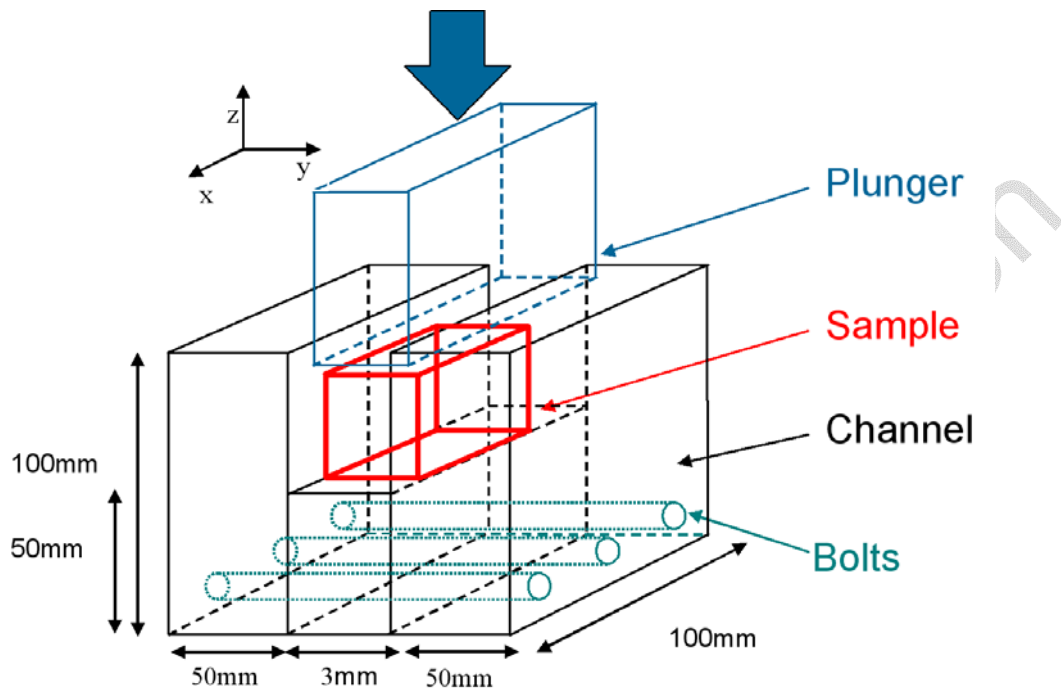


Fig. 1

Schematical drawing of the channel die plane strain set-up.

The rectangular samples exactly matched the channel geometry which was open in the longitudinal direction. The sample was compressed by a punch device permitting its unconstrained elongation along the longitudinal direction. The channel walls prevented lateral expansion during compression, leading to a macroscopic plane strain state. Solid-state lubrication was obtained by placing a Teflon foil of $80\text{ }\mu\text{m}$ thickness around the sample. The Teflon also protected the gray scale pattern on the sample surface required for the photogrammetric determination of the displacement field. Experiments were carried out at a strain rate of $1.7 \times 10^{-5}\text{ s}^{-1}$ and at room temperature. Plastic deformation proceeded in a series of subsequent steps each imposing a macroscopic engineering thickness reduction of about 3 - 5% per compression step. Crystal orientation maps and digital image pairs of the sample surface were taken after each of the subsequent plane strain deformation steps. The images

were used for the calculation of the three dimensional plastic displacement fields employing photogrammetry. Details of the method are outlined in the ensuing section.

2.2. Determination of the plastic displacement and strain fields

The determination of the plastic displacement field and the subsequent calculation of some tensor components of the plastic strain field was after each deformation step conducted by a photogrammetric procedure. This is a digital image analysis method which is based on the recognition of geometrical changes in the gray scale distribution of surface patterns before and after straining [1, 8]. Both, the natural characteristics of an unprepared sample surface or an artificial quasi-stochastic color spray applied to a polished surface (Fig. 2) may serve as input pattern. In order to measure the three dimensional surface coordinates digital stereo pair images of the sample were acquired using two high resolution CCD cameras as shown in Fig. 3.

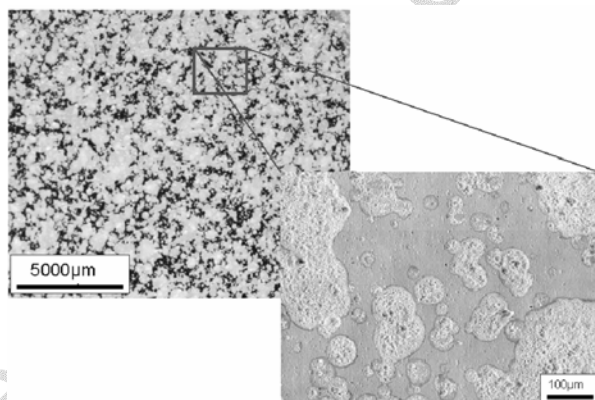


Fig. 2

Sprayed gray scale pattern on the surface of an undeformed polished and etched aluminium sample. The upper left picture was taken by digital optical microscopy. The lower right picture was taken in the scanning electron microscope. Images of this kind, taken before and after straining, were used for the photogrammetric calculation of the plastic displacement fields. For the spray a color was chosen which did not affect the orientation measurement via electron back scattering diffraction.

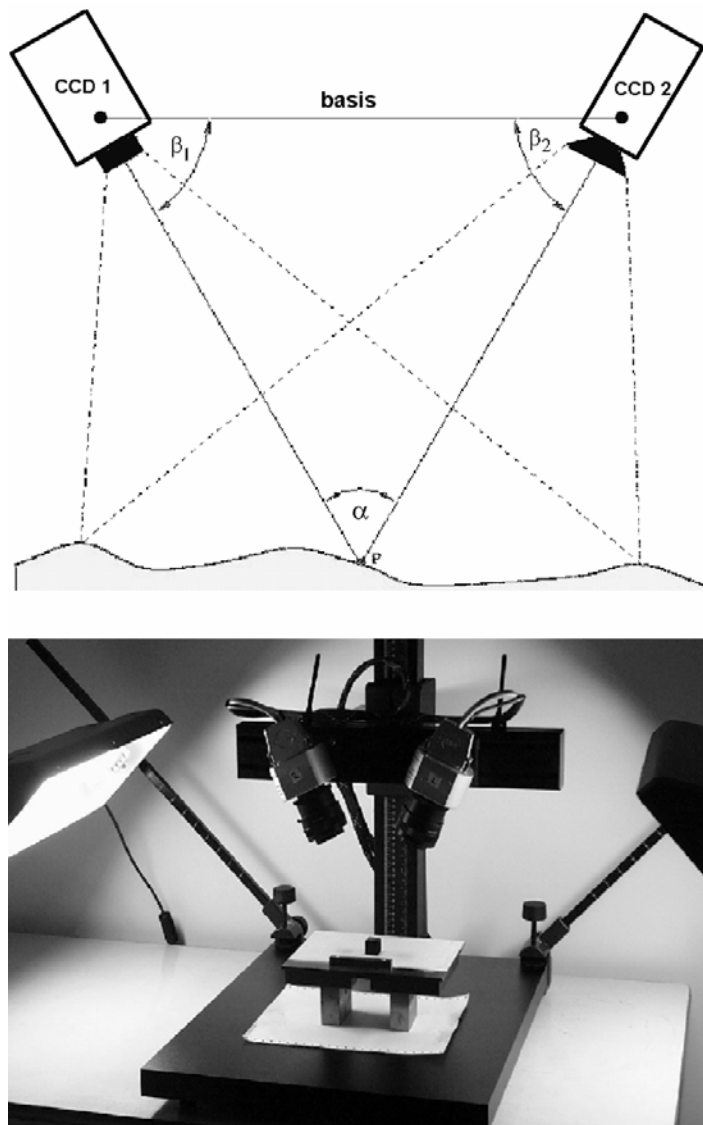


Fig. 3

Schematical drawing and photo of the experimental set-up of the CCD camera system.

Pattern recognition was carried out by a digital image processing procedure which maps a rectangular grid onto the image. The grid points are characterized by three dimensional coordinates and by the gray scale distribution in their proximity, Fig. 4. After straining the pattern is again recognized based on the assumption that the gray scale distribution around a certain coordinate remains constant during straining. From the change in border coordinates containing the correct initial gray scale distribution around the grid point the three dimensional displacement gradient tensor field is determined at each grid point. These data

serve as input for deriving the surface components of the local strain tensor. The strain tensor is used in the definition as the first order approximation of the standard polar decomposition of the displacement gradient tensor.

In this study a fine white color spray was applied to the polished surface of the undeformed sample. The resulting gray scale pattern on the surface of the specimen was recorded and reference coordinates for the different experimental methods (microtexture, metallography, microstrain determination) were fixed on the sample surface. These surface markers allowed us to identify the same sample areas under the different experimental environments ensuring a one-to-one correspondence of the different results. The specimen was then plane strain compressed using the channel die set-up. After each deformation step the surface gray scale pattern was acquired and the displacement gradient field as well as the strain distribution were calculated.

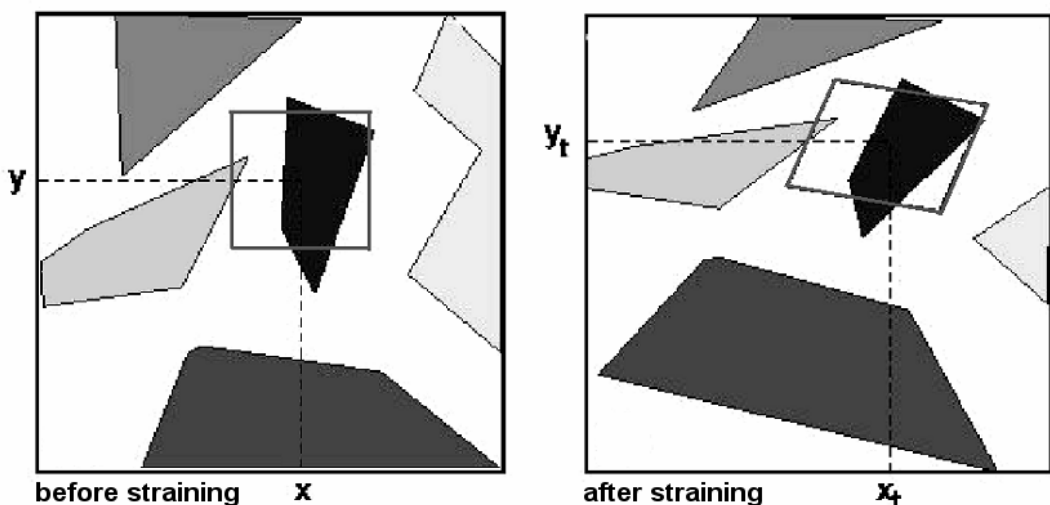


Fig. 4

Schematical drawing indicating the initial array (before straining) and the distorted array (after straining) containing a matching gray scale distribution.

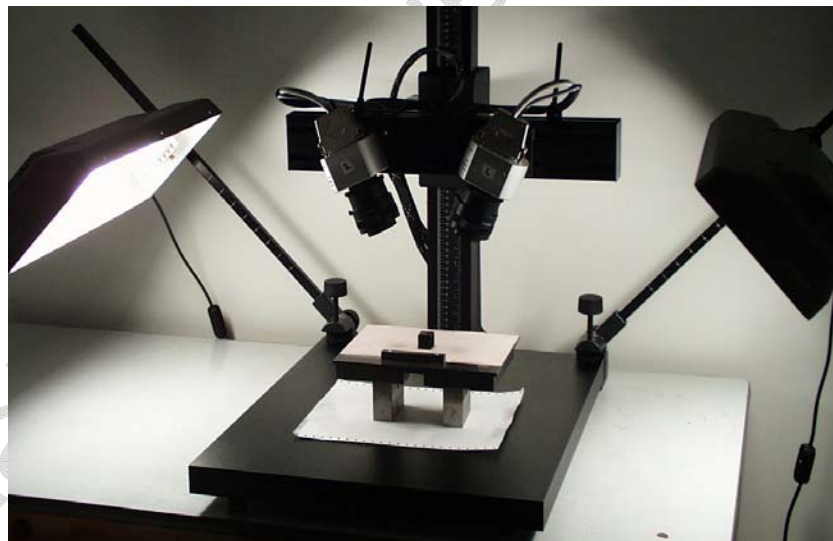
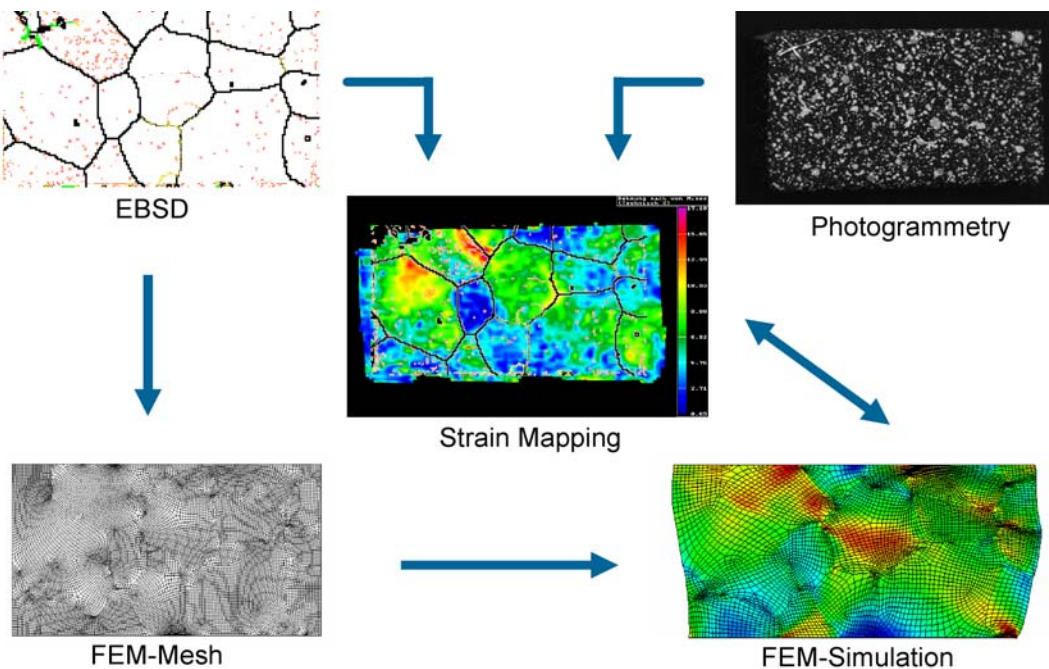


Fig. 5a

Principle of our joint experimental procedure

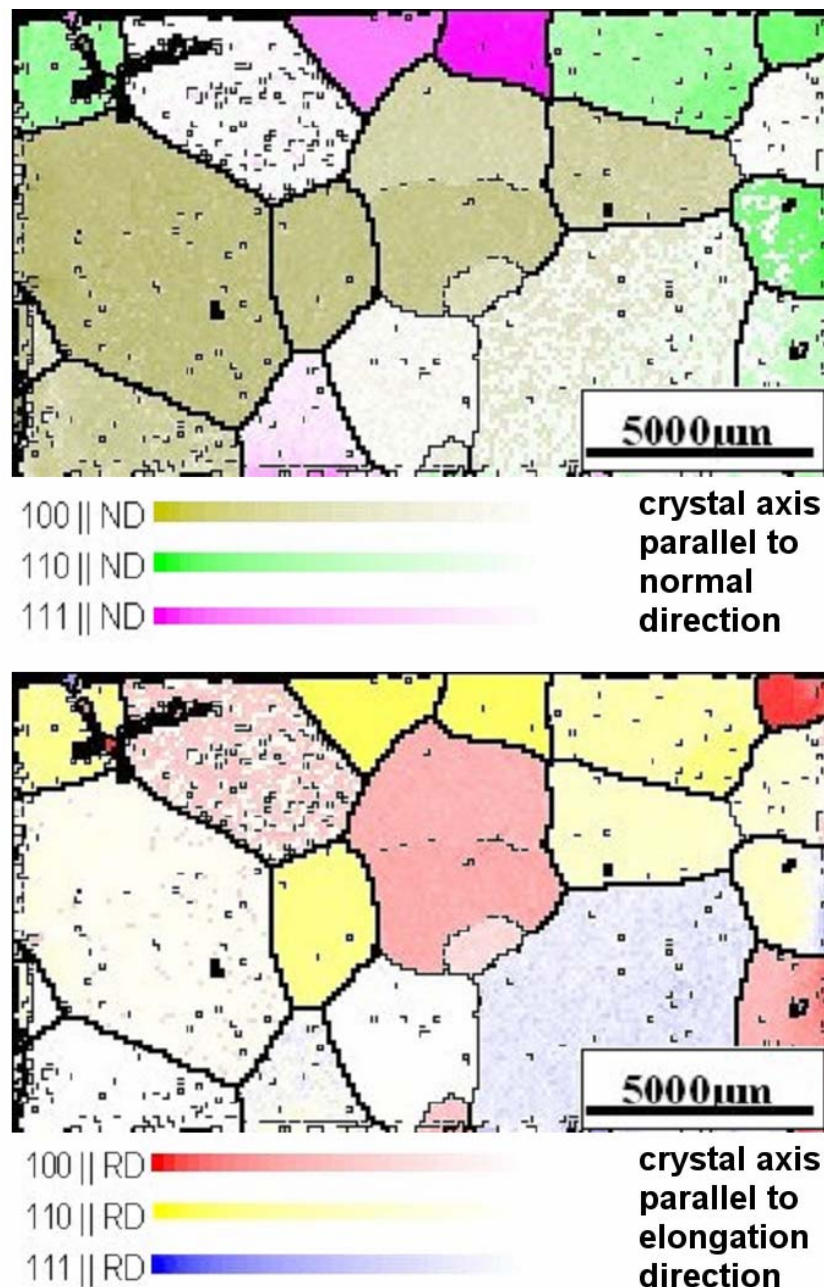


Fig. 5b

Crystallographic microtexture of the sample before plastic deformation using separate color scales for the crystallographic axes parallel to the direction normal to the compression axis (ND) and parallel to the extension direction (RD). The grain boundaries with orientation changes above 15° were superimposed on Fig. 6.

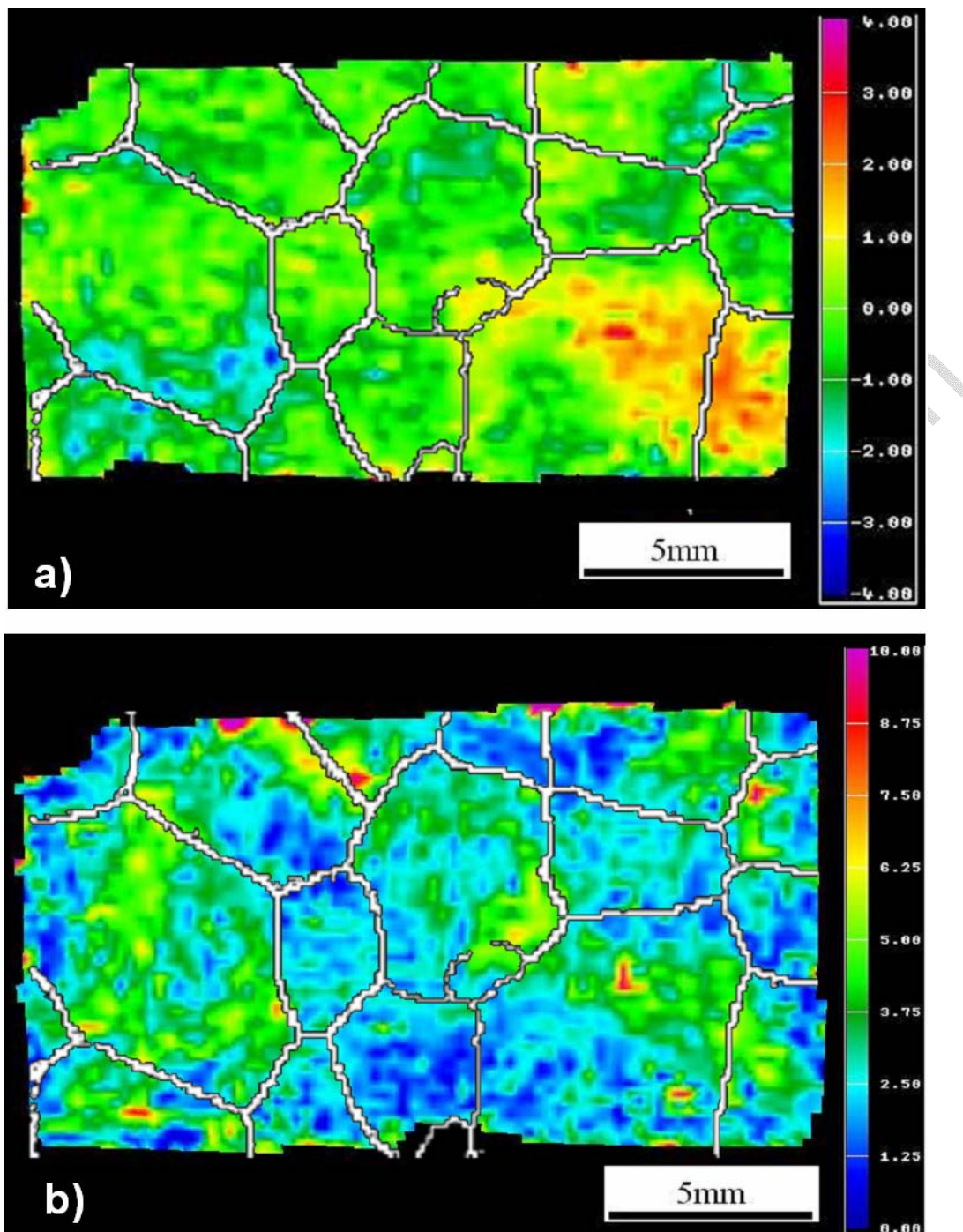


Fig. 6

Distribution of the (a) accumulated engineering plastic shear and (b) von Mises strain in the specimen after 3% sample thickness reduction ($\Delta d/d$, where d is the sample extension along compression direction). The strains were determined using photogrammetry. The grain boundaries indicated by white lines were taken from microtexture measurements.

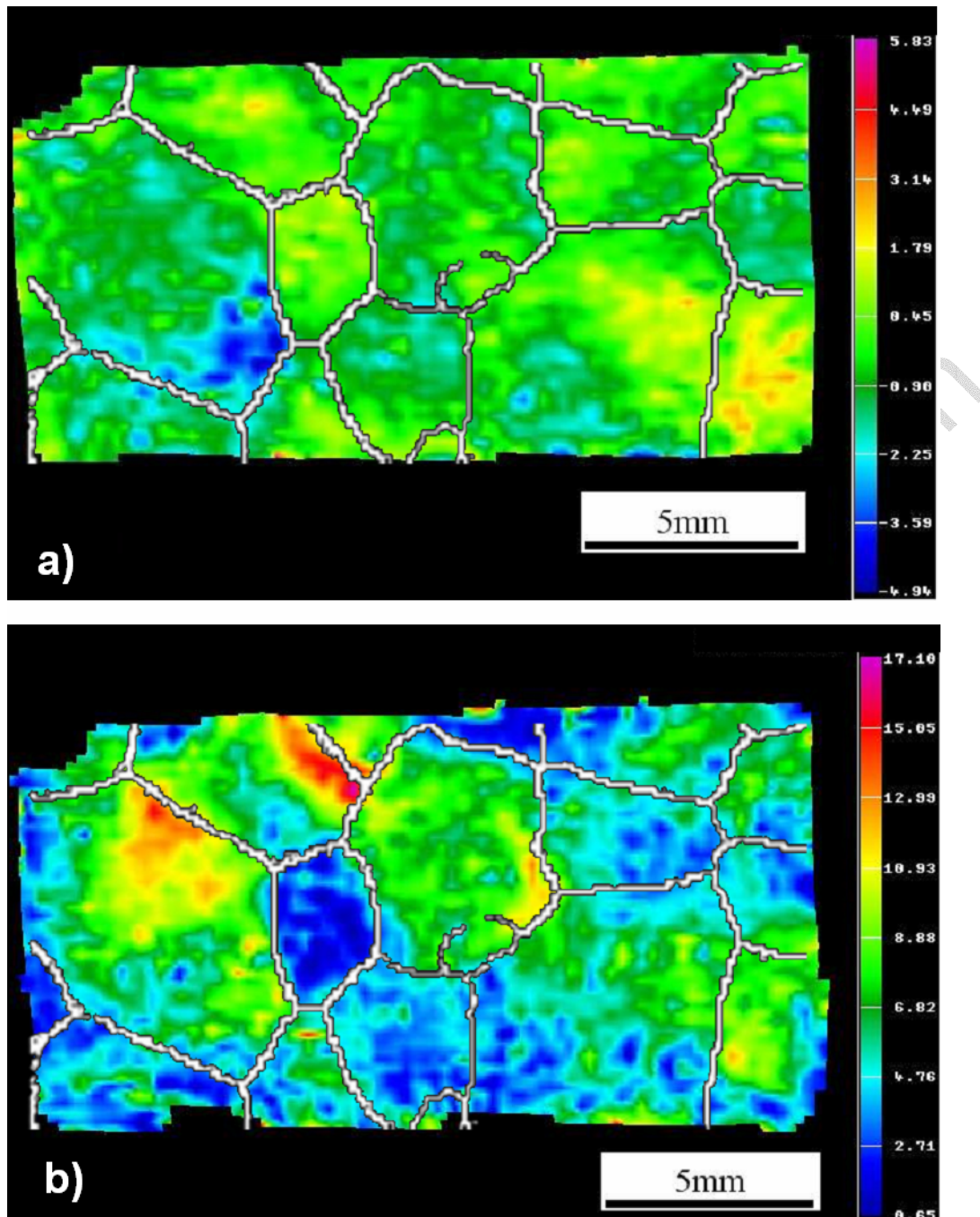


Fig. 7

Distribution of the (a) accumulated engineering plastic shear and (b) von Mises strain in the specimen after 8% sample thickness reduction ($\Delta d/d$, where d is the sample extension along compression direction). The strains were determined using photogrammetry. The grain boundaries indicated by white lines were taken from microtexture measurements.

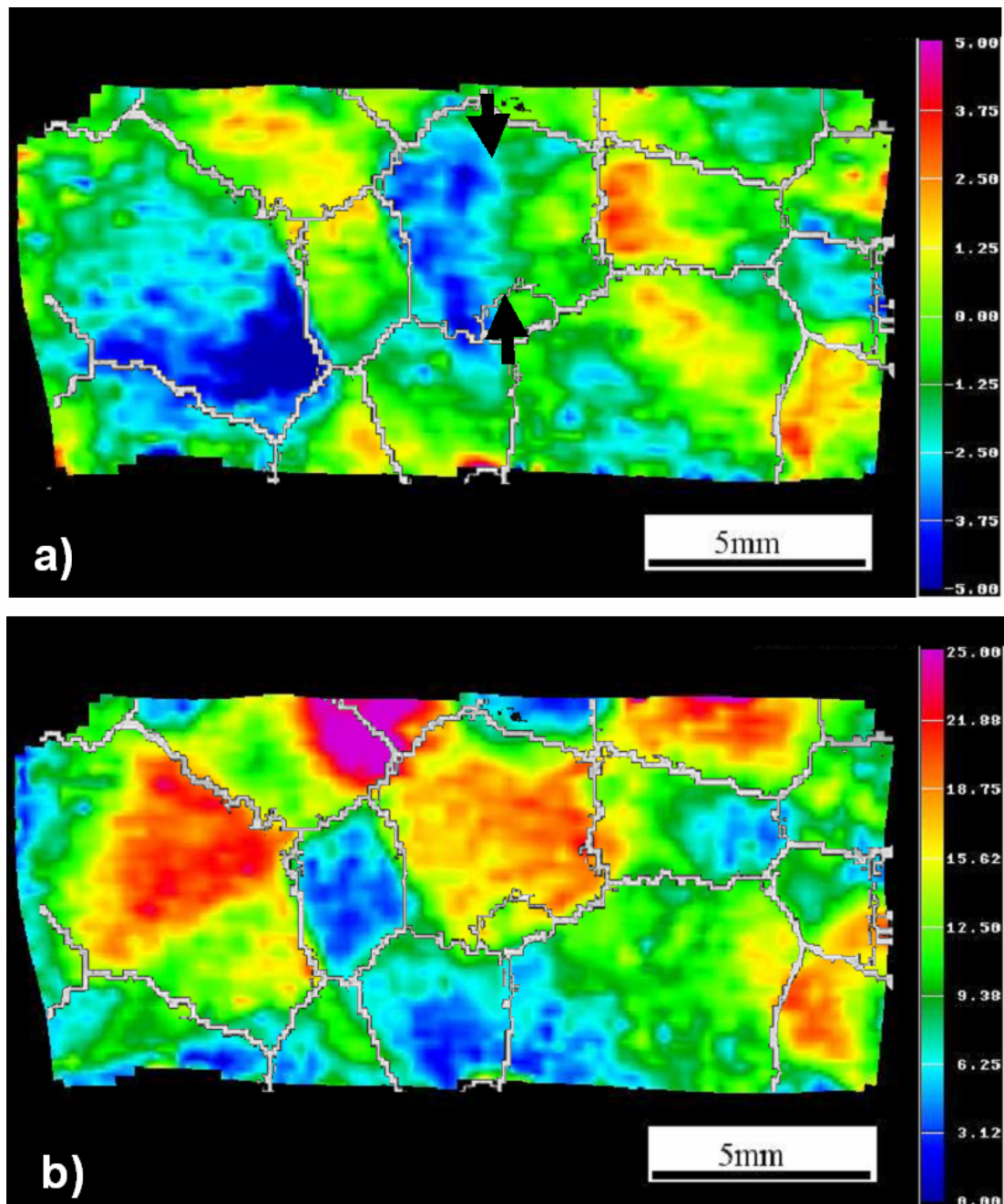


Fig. 8

Distribution of the (a) accumulated engineering plastic shear and (b) von Mises strain in the specimen after 15% sample thickness reduction ($\Delta d/d$, where d is the sample extension along compression direction). The strains were determined using photogrammetry. The grain boundaries indicated by white lines were taken from microtexture measurements.

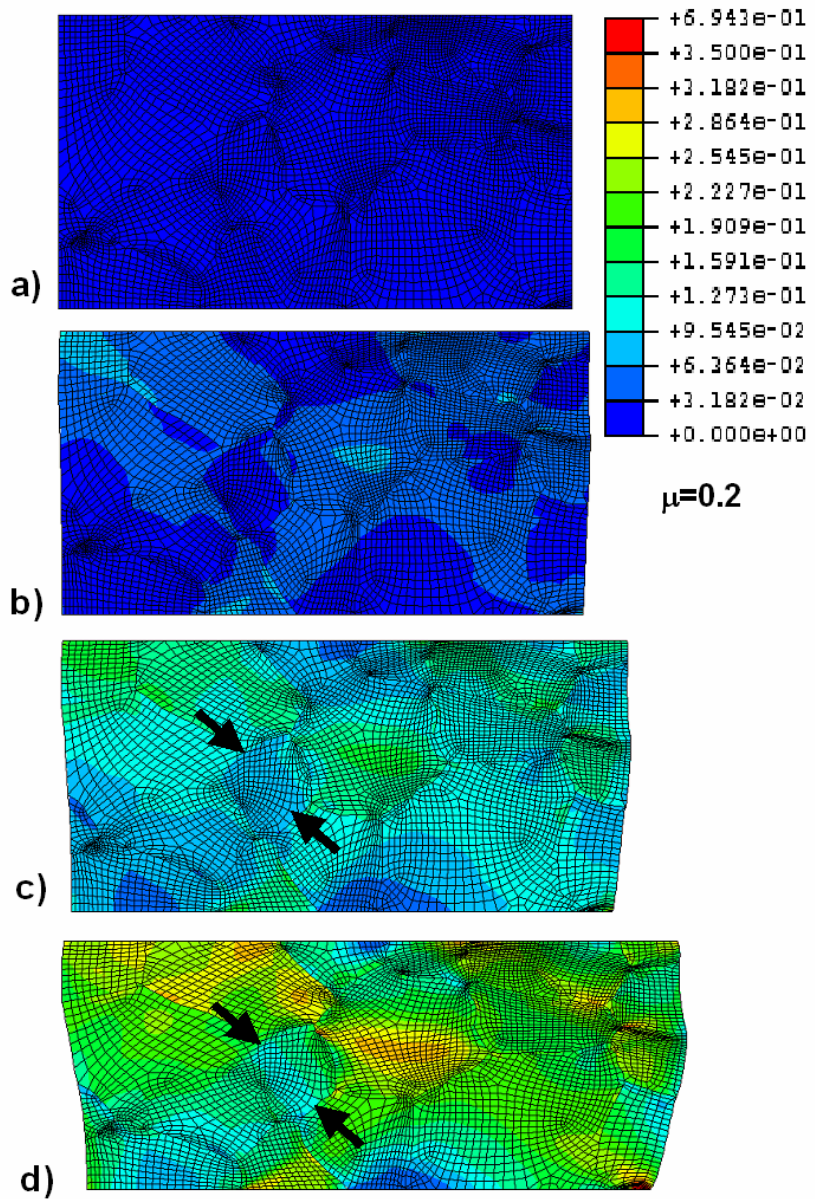


Fig. 9

- (a) The microstructure of the initial sample was mapped onto a finite element mesh. Grid configuration was conducted along the grain boundaries using a bilinear element with 4 nodes and 4 integration points (5705 elements).
- (b) - (c) Accumulated von Mises strain as predicted from the crystal plasticity finite simulation for 3 % (b), 8 % (c), and 15 % (d) sample thickness reduction. The finite element calculations were conducted using plane strain boundary conditions and a friction coefficient of $\mu=0.2$. The constitutive crystal plasticity law was implemented using 12 $\{1\bar{1}1\}<1\bar{1}0>$ slip systems and viscoplastic hardening. Finite element simulations were conducted using the finite element program ABAQUS in conjunction with the user defined material subroutine UMAT [14].

It must be underlined in this context that the photogrammetric method works without any additional artificial regular grid on the sample surface. The displacement gradient field is derived exclusively from changes in the border coordinates for a gray scale distribution at each coordinate. The spatial resolution of the method is therefore independent of some external grid size but is of the order of the respective optical setup (12.5 µm in the present case). The strain resolution is below 1% since the method uses the match of the complete gray scale distribution before and after loading as a measure to determine the exact shift in border coordinates. This procedure provides a larger precision than the determination of the new border coordinates in the form of discrete pixel steps.

Raabe - image correlation

3. Results and discussion

Using the experimental procedures described above two sets of mappings were determined after each deformation step, namely, the microstrain distribution and the microtexture.

Fig. 5 shows the microtexture of the undeformed polycrystalline sample. The upper diagram shows the orientation angles with respect to the crystal direction normal to the compression plane. The lower diagram shows the angles with respect to the extension direction.

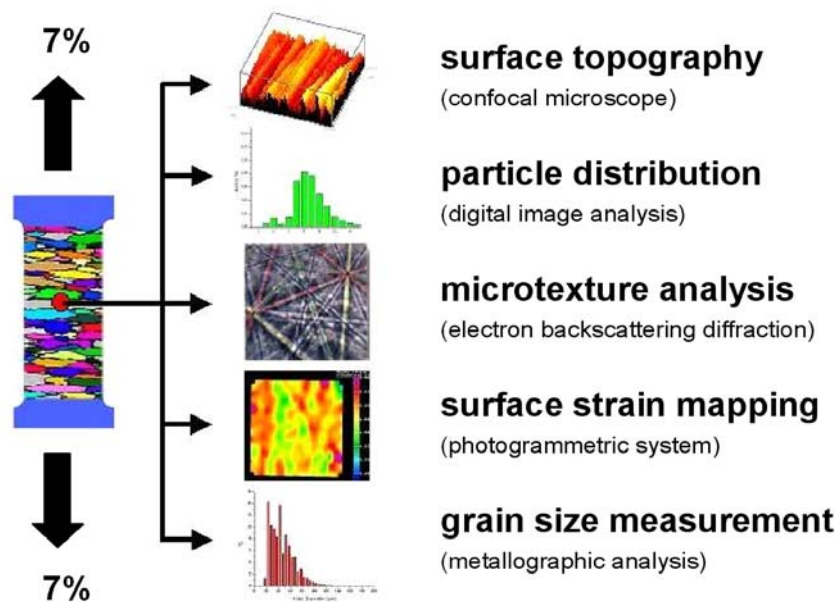


Fig. 10

Joint experimental strategy for one-to-one correlations.

Fig. 6(a) shows the in-plane distribution of the accumulated shear at the sample surface after 3% thickness reduction along the compression direction. The shear is given in the reference system of the sample formed by the compression direction and the longitudinal direction. The displacement fields were determined by use of the photogrammetric method explained in the preceding section. The experimentally determined grain structure (electron back scattering diffraction) is additionally mapped in the same diagram (Fig. 5). The superimposed lines indicate orientation changes above 15°. Fig. 6(b) shows the corresponding distribution of the accumulated von Mises strain together with the grain boundaries. The figures show that grain

scale deformation is nonuniform already at a very early stage of plastic straining. Pronounced localization of strain is initiated at some of the triple points and along some of the grain boundaries.

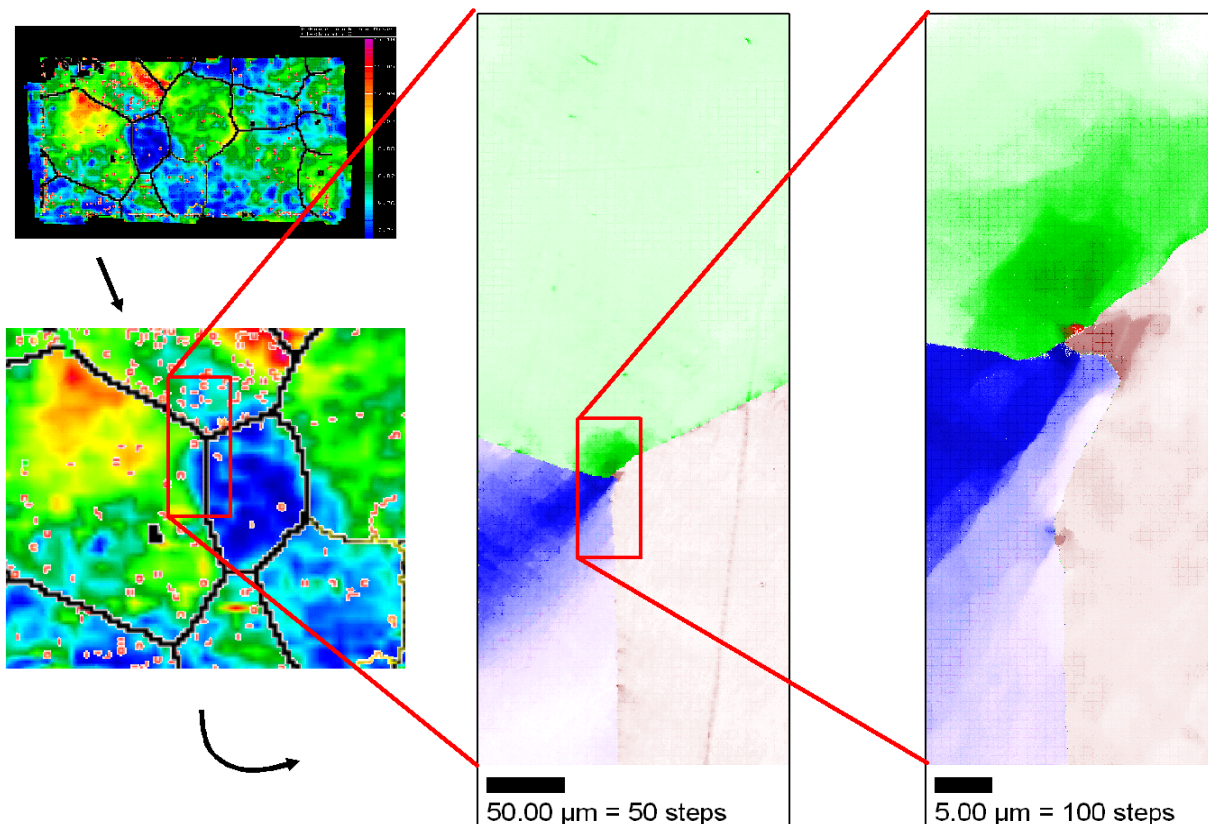


Fig. 11

Details of the strain measurement, right hand side shows the textures.

This tendency to accommodate the imposed strain in a heterogeneous fashion becomes even more obvious after 8% sample thickness reduction. Fig. 7 reveals that some grains show much higher accumulated plastic strain than others. While some crystals carry as little as 1% von Mises strain within their borders (Fig. 7b), others show maximum deformation above 16%, particularly close to the grain boundaries.

Some of the grains reveal a relatively homogeneous strain field inside their borders. This observation indicates that they respond as mechanical entities to the externally imposed load. Finding such homogeneous in-grain behavior is all the more surprising if one considers that

non-zero friction conditions always entail macroscopic strain gradients within the specimen [9]. As will be discussed below in more detail by use of crystal plasticity simulations we attribute this mechanically uniform response of some grains to the dominance of their orientation factors for the overall percolation path of the strain. It must be noted though that homogenization theory suggests smaller than the here observed variations in the strain distribution. The deviation between standard Taylor-Bishop-Hill-type polycrystal homogenization theory and the present observations can be readily attributed to the large grain size encountered in the present work. This means that a small set of large grains cannot be theoretically investigated using classical polycrystal models but must be treated using methods which more suited to treat the micromechanics of crystal clusters.

It is furthermore remarkable that strain gradients between 2% and 16% occur within some of the grains. The strain maximum occurs in such cases in front of large angle grain boundaries the plane of which have an inclination close to 45° relative to the reference sample system. Other pairs of grains reveal practically no change in strain across their common grain boundary. This applies particularly for boundaries with relatively small misorientation (below 15°). As a consequence, these grains seem to co-deform in a cluster-type fashion. However, due to the limited number of grains and grain boundaries involved in the present experiment it is not reasonable to draw general conclusions about grain cluster mechanics at this stage.

Similar tendencies are found after 15% total sample thickness reduction (Fig. 8). The changes in the accumulated strains from grain to grain are even more pronounced than at lower deformation. About half of the grains still behave as relatively homogenous mechanical units (Fig. 8(b)). This indicates that grain scale strain hardening has not yet led to an equilibration of the flow stress in all parts of the specimen. These continuing differences in grain hardness entail further amplification of grain-scale strain patterning. It is noteworthy that non-crystallographic strain localization effects do not dominate the appearance of strain heterogeneity in the sample. This observation underlines the strong importance of the initial crystal orientation distribution and the resulting profile in kinematic hardness for the overall strain heterogeneity.

Fig. 8(a) reveals another interesting detail, namely, the strong influence of the free surface on deformation. For instance the large grain in the center of the sample (see arrows) is separated into two areas, one revealing forward shear and the other one backward shear. This

orientation of shear in the direction of the closest free surface leads to an additional source of strain heterogeneity.

Due to the complexity of the experimental observations it is useful to inspect the situation under investigation by corresponding simulations. For this purpose we used a crystal plasticity finite element method. This technique accounts for the discrete crystallographic nature of in-grain and grain-to-grain polycrystal kinematics and allows one to conduct forming simulations with boundary conditions which approximate those of the real experiment.

For implementing crystal plasticity into a non-linear finite element scheme we used the fully-implicit time-integration method suggested by Kalidindi et al. [10]. This model provides a direct means for updating the material state via integration of the evolution equations for the crystal lattice orientation and the critical resolved shear stress. The deformation behavior of the grains is at each integration point determined by a crystal plasticity model which accounts for plastic deformation by crystallographic slip and for the rotation of the crystal lattice during deformation. The crystal kinematics follow those described by Asaro [11] and the rate-dependent formulation follows that developed by Peirce et al. [12, 13]. In this concept of the constitutive description the slip rate on a slip system is assumed to be related to the resolved shear stress on this system through a power law relation which is equipped with a scalar scaling parameter for the stress as a phenomenological measure for the slip system strength or resistance to shear and a strain rate sensitivity exponent of 0.002. The value of the strain rate sensitivity exponent is low so that the material response is practically rate-independent.

With the slip rates given as an explicit function of the known resolved shear stresses, the rate-dependent method avoids the ambiguity in the selection of active slip systems which is encountered in many rate-independent formulations where it must be solved using an additional selection criterion. For the present simulations, the strengths of all of the slip systems at a material point are taken to be equal, i.e. we adopt the Taylor hardening assumption. The hardening as a function of accumulated slip is assumed to follow the macroscopic strain hardening behavior obtained from a mechanical test by fitting the experimental data to a Voce equation. The fit was adjusted by the average Taylor factor, using an approximate value of 3, to give the slip system resistance to shear as a function of the accumulated shear. When applied in a polycrystal simulation of a tensile test, this treatment of the slip system hardening will approximately reproduce the hardening behavior which was

originally measured. The cubic elastic constants used in the simulation are typical for aluminum: $C_{11} = 108 \text{ GPa}$, $C_{12} = 62 \text{ GPa}$ and $C_{44} = 28.3 \text{ GPa}$. Further details on the simulations are given in [1].

The microstructure of the initial sample was mapped onto an appropriate finite element mesh, Fig. 9(a) [13]. Grid configuration was conducted along the grain boundaries employing a bilinear element with 4 nodes and 4 integration points using 5705 elements. The finite element calculations were conducted under external plane strain boundary conditions using a friction coefficient of $\mu=0.2$. The constitutive crystal plasticity law was implemented with 12 $\{1\bar{1}1\}<110>$ slip systems. Finite element simulations were conducted using the finite element program ABAQUS in conjunction with the user defined material subroutine UMAT [14].

Figs. 9(b)-(d) show the accumulated von Mises strain as predicted from the crystal plasticity finite simulation for 3%, 8%, and 15% sample thickness reduction. The simulations show a very heterogeneous distribution of strain, similar as observed experimentally. In some areas they show a strain pattern which reproduces the topology given by the large angle grain boundaries. This is accord with the experimental observations (e.g. for 8% thickness reduction see Figs. 6(b) and 9(c)). Pronounced strain localization occurs along the upper left and lower right parts of the deformed shape diagonals as well as within the center grains (e.g. Fig. 9(c)). Areas with small plastic strain can be found in the vicinity of the middle of the top and bottom edges. Some grains reveal very small overall strains within their borders (see arrows in Figs. 9(c),(d)).

The simulations reveal a good agreement with the experiments. Deviations can essentially be attributed to the friction conditions and their change during forming (the simulations assumed constant friction conditions). The major correspondence of the simulations and the experiments is that grain scale heterogeneity is mainly determined by two factors. First, by the external friction conditions. Second, by the occurring orientation factors and their influence on strain accommodation.

4. Conclusions

The paper presented a novel experimental approach for the investigation of grain-scale strain heterogeneity during plastic deformation. The main results are:

- Quantitative experimental grain- and sub-grain scale strain analysis can be conducted using photogrammetry in conjunction with microtexture experimentation.
- Strain patterning in aluminum during plane strain compression is strongly determined by the orientation dependence of the kinematic hardness of the individual grains. This effect was interpreted in terms of the respective orientation factors.
- Two forms of grain deformation were observed. The first kind was characterized by the individual and homogeneous deformation of single grains at individual strain levels (corresponding to their orientation factors) which were significantly different from those of their neighbor grains. The second kind was characterized by the co- or cluster-type deformation of areas comprising more than one grain, revealing a common fairly homogeneous strain level.
- At sample thickness reductions up to 3% strain localization was in some cases initiated at grain triple points (the specimen had a quasi 2D columnar grain structure) and along some grain boundaries which had an angle close to 45° with respect to the sample coordinates.
- The experimental results were in good accord with corresponding crystal plasticity finite element simulations.

References

1. D. Raabe, M. Sachtleber, Z. Zhao, F. Roters, S. Zaefferer: *Acta Mater.* 49 (2001) 3433.
2. F. Delaire, J. L. Raphanel, C. Rey, *Acta Mater.* 48 (2000) 1075.
3. C. Lineau, C. Rey, P. Viaris, *Mater. Sc. Eng.* A234-236 (1997) 853.
4. S. V. Harren, R. J. Asaro, *J. Mech. Phys. Solids* 37 (1989) 191.
5. A. J. Beaudoin, H. Mecking, U. F. Kocks, *Phil. Mag. A* 73 (1996) 1503.
6. R. C. Becker, S. Panchanadeeswaran, S., *Acta Metall.* 43 (1995) 2701.
7. K. K. Mathur, P. R. Dawson, *Int. J. Plast.* 8 (1998) 67.
8. Handbook for the Aramis system by GOM mbh, Gesellschaft für Optische Meßtechnik, Version September 2000, Braunschweig, Germany
9. D. Raabe, Z. Zhao, S.-J. Park, F. Roters: *Acta Materialia* 50 (2002) 421–440
10. S. R. Kalidindi, C. A. Bronkhorst, L. Anand, *J. Mech. Phys. Solids* 40 (1992) 537.
11. R. J. Asaro, *Adv. appl. Mech.* 23 (1983) 1.
12. D. Peirce, R. J. Asaro, A. Needleman, *Acta Metall.* 31 (1983) 1951.
13. H. Weiland, R. C. Becker, in: T. Leffers and O. P. Pederson (Eds.), *Proceedings 20. RISØ International Symposium on Materials Science*, RISØ National Laboratory, Roskilde, Denmark, 1999, p. 213.
14. ABAQUS/Standard User's Manual, Volume II, 14.1.4-1, , Hibbit, Karlsson and Sorensen (Publ.), Pawtucket, RI, USA, 1999.
15. M. Sachtleber, Z. Zhao, D. Raabe: *Materials Science and Engineering A* 336 (2002) 81–87,